NANO LETTERS

LETTER

pubs.acs.org/NanoLett

Nanoengineering the Heart: Conductive Scaffolds Enhance Connexin 43 Expression

Jin-Oh You, Marjan Rafat, George J. C. Ye, and Debra T. Auguste*

School of Engineering and Applied Sciences, Harvard University, Cambridge, Massachusetts 02138, United States

Supporting Information

ABSTRACT: Scaffolds that couple electrical and elastic properties may be valuable for cardiac cell function. However, existing conductive materials do not mimic physiological properties. We prepared and characterized a tunable, hybrid hydrogel scaffold based on Au nanoparticles homogeneously synthesized throughout a polymer templated gel. Conductive gels had Young's moduli more similar to myocardium relative to polyaniline and polypyrrole, by 1−4 orders of magnitude. Neonatal rat cardiomyocytes exhibited increased expression of connexin 43 on hybrid scaffolds relative to HEMA with or without electrical stimulation.

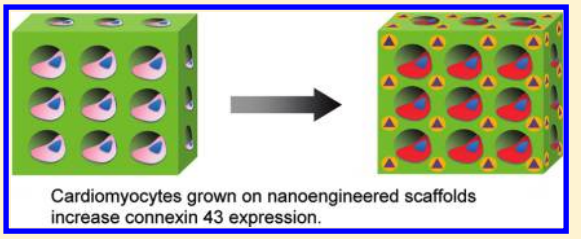

KEYWORDS: Scaffold, cardiomyocyte, conductive, Au nanoparticles, HEMA, connexin 43

Cardiac disease is often associated with abnormalities in electrical function that can severely impair cardiac performance. In many arrhythmias, slow conduction and unidirectional conduction block result from insufficient intercellular electrical coupling at gap junctions.[1] We hypothesized that electrically active scaffolds may be used to improve cardiomyocyte function by increasing connexin 43 (Cx43) expression.

Scaffolds provide the basic, mechanical platform for engineering a tissue. Scaffolds with similar chemical and mechanical properties to native tissue have been engineered to improve cell adhesion, viability, proliferation, and function.[2−5] Scaffolds designed to mimic cardiac tissue in both stiffness and anisotropy have shown improvements in cardiomyocyte electrical excitation and gap junction formation.[6,7]

External electrical fields have also been applied to cell-laden scaffolds to regulate the biophysical properties of cells in vitro; increased fibroblast proliferation,[8,9] neurite extension,[10,11] stem cell differentiation,[12,13] and cardiac synchronization[14] have been observed. Conducting polymers like polyaniline (PANI) and polypyrrole (PPy), which fail to mimic physiological moduli, have been shown to support the attachment and proliferation of various mammalian cell lines such as myoblasts,[15] fibroblasts,[16] and endothelial cells.[17] Scaffolds that couple electrical, mechanical, and chemical considerations may provide the appropriate environmental stimuli to foster healthy cell function and tissue formation.

Electrically conductive scaffolds were prepared by a two-stage synthesis as described in Scheme 1. First (Scheme 1A), thiol-2-hydroxyethyl methacrylate (thiol-HEMA) was synthesized by dodecylthiol ether end functionalization of HEMA using dodecanethiol (DDT) and 2,2′-azobisisobutyronitrile (AIBN).[18] Synthesized thiol-HEMA was mixed with HEMA at different mass to volume ratios and poured into a close-packed lattice of poly(methyl methacrylate) (PMMA) microparticles (average diameter 200 μm) on concave glass. Figure 1A shows an optical microscopy image of PMMA microparticles for making close-packed lattices. The thiol-HEMA/HEMA solution was cross-linked by tetra(ethylene glycol) dimethacrylate (TEGDMA) and photopolymerized under UV light using AIBN as the photoinitiator. Figure 1B depicts the polymerized hydrogels with embedded PMMA particles. Porous scaffolds were obtained by removing the embedded PMMA microparticles in dichloromethane (DCM) (Figure 1C). The scaffolds were made conductive (Scheme 1B) by immersion into aqueous potassium tetrachloroaurate ($KAuCl_4$). Au nanoparticles within the scaffolds were obtained by reduction in sodium borohydride ($NaBH_4$) due to the affinity of both colloidal Au and Au^{3+} ions with thiol groups. Panels D−H of Figure 1 depict scaffolds with increasing amounts of thiol-HEMA. As the thiol-HEMA content increased from 0 to 40% (thiol-HEMA weight/HEMA volume, w/v) relative to the HEMA solution, the color of the scaffolds appeared darker, signifying an increase in Au content. Scaffold dimensions were 8 mm in diameter by 1 mm in thickness.

Au nanoparticles were homogenously dispersed throughout the thiol-HEMA/HEMA scaffolds as shown in the transmission electron microscopy (TEM) images (Figure 2A,B). The average particle sizes of scaffolds incorporating 10 and 40% (w/v) thiol-HEMA were 8.1 ± 0.9 and 4.4 ± 0.3 nm, confirmed by particle size analysis using ImageJ (NIH) and TEM. Au nanoparticles remained evenly distributed in scaffolds placed in deionized water for >180 days. As shown in Figure 2C, absorption spectra for 1, 10, 20, and 40% (w/v) thiol-HEMA/HEMA confirmed the decreasing Au nanoparticle size with increasing thiol-HEMA content. The UV−vis traces have an absorption maximum near 525 nm, which is characteristic of the surface plasmon resonance of well-spaced Au nanoparticles.[19−21] At low Au content (1 and

Received: May 6, 2011
Revised: July 14, 2011
Published: August 01, 2011

Scheme 1. Illustration of (A) the Synthesis of thiol-HEMA and (B) Reduction of Au within the thiol-HEMA/HEMA Scaffold

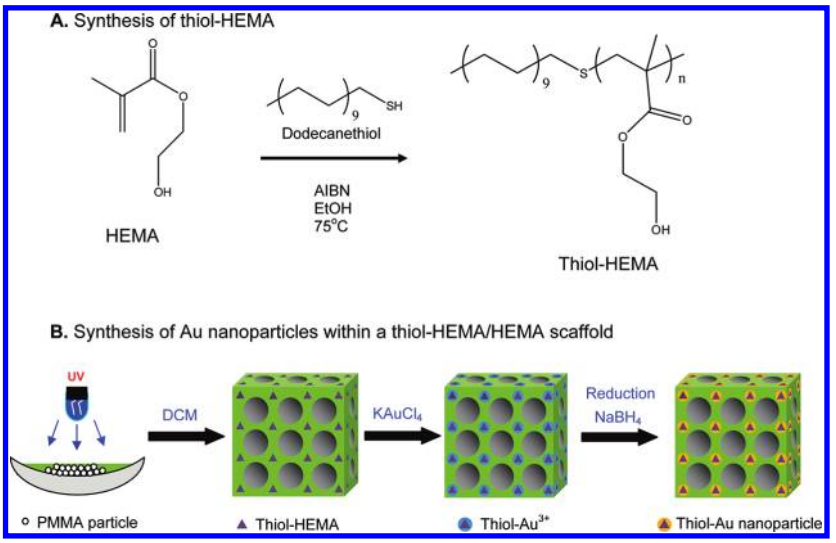

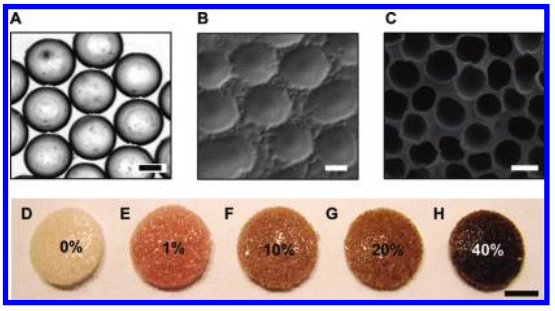

Figure 1. Preparation of conductive scaffolds. (A) Optical micrograph of PMMA microspheres used to form lattices. (B) SEM image of a HEMA hydrogel with embedded PMMA microparticles. (C) SEM image of Au impregnated HEMA scaffold after removal of PMMA particles. Optical images of porous HEMA scaffold (D) and Au impregnated HEMA scaffolds with varying thiol-HEMA content, 1 (E), 10 (F), 20 (G), and 40% (w/v) (H), respectively. The scale bars are 100 μm (A, B), 200 μm (C), and 3 mm (D−H).

10% w/v), the absorbance between 600 and 700 nm was high, indicating the aggregation of Au particles. The absorption spectra confirmed the presence of homogeneous, monodisperse Au nanoparticles at 40% (w/v). The amount of thiol-HEMA in the scaffolds regulated Au nanoparticle size and number.

The mass of Au was a function of the thiol-HEMA content. Thermogravimetric analysis (TGA) showed a mass loss region between 220 and 440 °C for HEMA and Au nanoparticle impregnated thiol-HEMA/HEMA scaffolds (Table S1, Supporting Information). The thermogram demonstrated that 40% (w/v) thiol-HEMA/HEMA scaffolds were composed of 3.4 ± 0.2 wt % of Au nanoparticles. In contrast, only 0.22 ± 0.01 wt % of Au nanoparticles was observed in the 10% (w/v) thiol-HEMA/HEMA scaffolds. The mass of thiol-HEMA correlated with the mass of Au embedded within the scaffolds.

A physiologically relevant Young's modulus is also desired for cardiac scaffolds; cardiac cells grow best on soft materials like polyacrylamide[22] or fibrinogen.[23] Conductive thiol-HEMA/HEMA scaffolds were measured under tensile stress on an Instron BioPuls 5543 machine (Instron, Norwood, MA). A representative stress−strain curve is shown for 0% w/v thiol-HEMA scaffolds in Figure 2D. As shown in Figure 2E, the Young's moduli increased with decreasing thiol-HEMA content from 600 to 1600 kPa. The scaffolds had mechanical properties that were stiffer than native heart muscle, which is comprised primarily of collagen and is elastomeric with a stiffness of approximately 50−100 kPa during diastole.[6,22,24−26] The modulus of active myocardium during systole, however, is approximately 20-fold higher, which more closely resembles the thiol-HEMA/HEMA scaffold moduli.[27,28] In addition, thiol-HEMA/HEMA scaffolds are 1−4 orders of magnitude softer than PANI[15,16,29,30] and PPy[31,32] conductive biomaterials, which have Young's moduli ranging from 6 to 10000 × 10^3 kPa. Table S2 (Supporting Information) provides the mechanical properties of various materials used either for cardiac tissue engineering or for conductive scaffolds. Mechanical[6,33] or chemical[34,35] cues may be used with our hybrid materials to couple the increased Cx43 expression with cellular organization. Future scaffold designs should incorporate anisotropy to more closely resemble the native myocardium as anisotropy has been shown to enhance cardiac function.[7]

Four Au impregnated scaffolds, comprised of 0, 10, 20, and 40% (w/v) thiol-HEMA, were measured for conductivity (Figure 2F) using a Keithley programmable current source and electrometer (Keithley Instruments, Inc., Cleveland, OH). The electrical conductivity of the Au impregnated, 40% (w/v) thiol-HEMA scaffolds was 15.3 ± 0.8 S/m. This was 30% higher than HEMA scaffolds, which had a conductivity of 10.6 ± 0.6 S/m. The conductivity observed in thiol-HEMA/HEMA scaffolds was high with respect to physiological values but comparable to typical conductive hydrogel values between 0.1 and 30 S/m.[36−38] The conductivity of intracellular and extracellular tissues (ventricular muscle, blood, lung, and skeletal muscle) ranged from 0.03 to 0.6 S/m.[39] Scaffold conductivity was controlled by altering the thiol-HEMA content.

Electrically conductive and elastic thiol-HEMA/HEMA scaffolds were incubated with fibronectin (25 μg/mL for 1 h) prior to seeding with 5 × 10^5 neonatal rat cardiomyocytes per scaffold. Cardiomyocytes were cultured for 3 days to allow for strong adhesion. This was followed by 5 days of electrical stimulation at

dx.doi.org/10.1021/nl201514a |*Nano Lett.* 2011, 11, 3643–3648

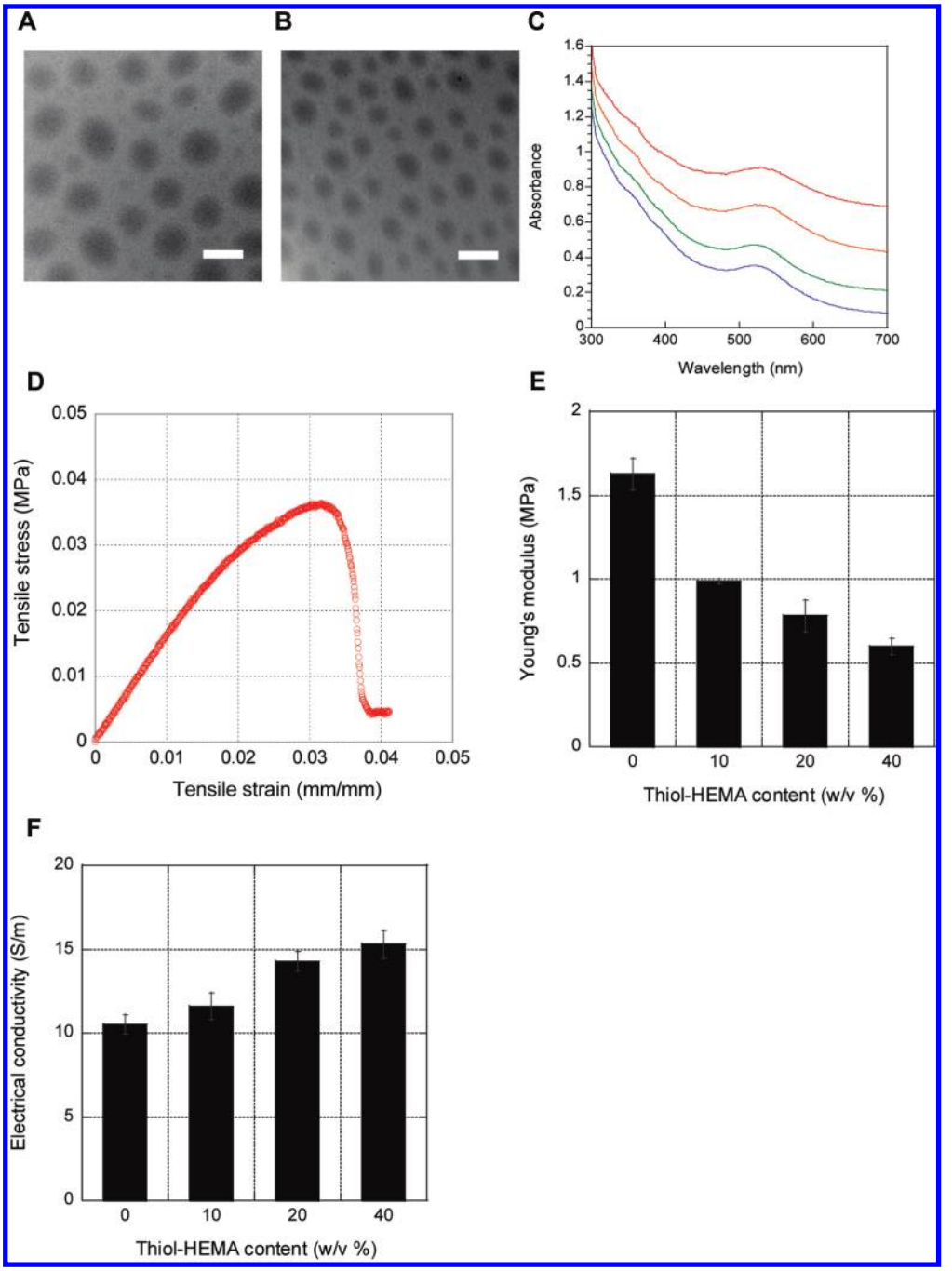

Figure 2. Characterization of Au impregnated thiol-HEMA/HEMA scaffolds. TEM images of Au nanoparticles in (A) 10 and (B) 40% (w/v) thiol-HEMA/HEMA scaffolds. Scale bar is 10 nm. (C) UV−vis spectra of Au impregnated thiol-HEMA/HEMA scaffolds in deionized water with increasing thiol-HEMA content: 1 (red), 10 (orange), 20 (green), and 40% (w/v) (blue), respectively. (D) Representative stress−strain curve for 0% (w/v) thiol-HEMA scaffolds. (E) Young's moduli of HEMA scaffolds with increasing thiol-HEMA content. (F) Conductivity of Au impregnated thiol-HEMA/HEMA scaffolds with increasing thiol-HEMA content. Error bars represent standard error with $n = 5$.

2 mA rectangular pulses (2 ms, 1 Hz, 5 V/cm). Cardiomyocyte viability was measured using the alamarBlue assay. Figure 3A illustrated that unstimulated cells maintained their viability after 8 days of culture regardless of scaffold thiol-HEMA content. After electrical stimulation (Figure 3B), cardiomyocyte viability showed an increasing trend with increasing thiol-HEMA content; however, statistical significance was not observed.

Cardiomyocyte-laden scaffolds were evaluated by scanning electron microscopy (SEM) (Figure 4). SEM images of unstimulated (Figure 4A,C) and stimulated (Figure 4E,G) cardiomyocytes revealed clustering within scaffold pores. Cardiomyocytes were observed as clusters and single cells on all scaffolds independent of the thiol-HEMA content or stimulation condition. Cardiomyocyte beating was observed on all scaffolds after 5 days of culture (Supplementary Movie 1, Supporting Information).

Cx43 was evaluated to identify whether a conductive scaffold and electrical stimulation could increase expression. Cardiomyocytes express multiple connexins, proteins that form gap junction

dx.doi.org/10.1021/nl201514a |*Nano Lett.* 2011, 11, 3643–3648

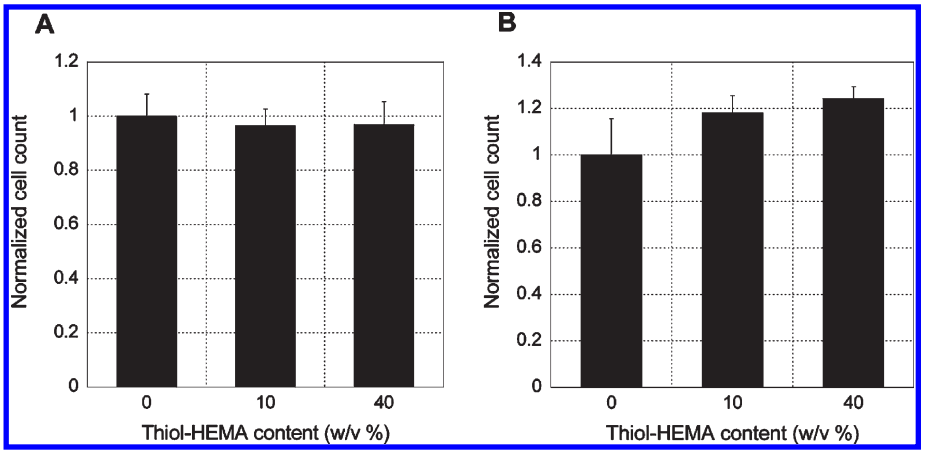

Figure 3. Cardiomyocyte viability. Cardiomyocytes seeded on thiol-HEMA/HEMA scaffolds were assessed by the alamarBlue assay for unstimulated (A) and stimulated (B) conditions. Cells were stimulated with 2 mA rectangular pulses (2 ms, 1 Hz, 5 V/cm) for 5 days after 3 days of initial seeding at 5×10^5 cells/scaffold. Data are reported as a normalized cell count, where the cell numbers were normalized to the 0% w/v thiol-HEMA condition. Error bars represent the standard error from three independent scaffolds tested per condition.

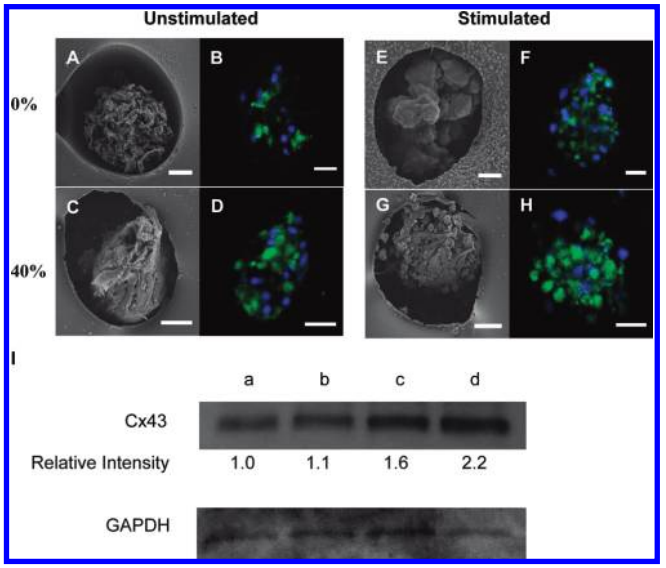

Figure 4. Cell morphology and connexin 43 (Cx43) expression. Unstimulated (A−D) and stimulated (E−H) cardiomyocytes were observed on scaffolds with 0 (A, B and E, F) and 40% (w/v) thiol-HEMA/HEMA (C, D and G, H). SEMs (A, C, E, and G) depict that cardiomyocytes cluster within pores. Nuclear and Cx43 stains are shown in blue and green, respectively (B, D, F, and H). Scale bar is 25 μm. (I) Western blot analysis of Cx43 expression in unstimulated (a and c) and stimulated (b and d) scaffolds with 0% (a and b) and 40% w/v (c and d) thiol-HEMA content. GAPDH was evaluated to verify loading efficiency. Protein expression was quantified through evaluating the relative intensity of the Cx43 bands normalized to the 0% w/v thiol-HEMA unstimulated condition.

channels that regulate how current spreads from one cardiomyocyte to another. Mice heterozygous for the Cx43 null mutation ($Cx43^{+/-}$ mice) exhibited a 50% loss in Cx43 expression, resulting in a 40% reduction in ventricular conduction velocity.[40] Therefore, loss of Cx43 expression has been linked with impeding electrical signaling between cells. Immunofluorescence staining was conducted to confirm the presence of Cx43 on unstimulated (Figure 4B,D) and stimulated (Figure 4F,H) scaffolds. To verify changes in protein expression, a Western blot analysis was performed (Figure 4I). The amount of Cx43 was observed to be 2-fold higher in stimulated samples containing 40% w/v thiol-HEMA in comparison to nonconducting scaffolds (Figure 4Ib vs Figure 4Id). Surprisingly, Cx43 expression was also significantly higher (60%) when cells were seeded on electrically active scaffolds without electrical stimulation relative to nonconducting scaffolds without stimulation (Figure 4Ia vs Figure 4Ic).

Cx43 has been shown to regulate cell−cell communication, influence electrical coupling, and promote contractile behavior.[41−43] The enhanced expression of Cx43 suggested that cardiomyocytes may be stimulated when seeded on electrically active scaffolds. Elevated levels of Cx43 have previously been reported after electrical stimulation on collagen scaffolds compared to unstimulated controls.[44] Amplification of Cx43 due to matrix conductivity opens new doors to the ability of cardiac cells to sense and respond to their environment. Factors such as substrate stiffness[3−5] and surface chemistry[45−47] have been implicated previously in determining cell morphology, fate, and migration.

Coupling Au nanoparticles with the transparency, elasticity, and chemical versatility of a hydrogel yields control over the chemical, mechanical, and conductive properties of the cell microenvironment. The hybrid scaffold design was based on a polymer templating technique which allows for the homogeneous synthesis of Au nanoparticles throughout the gel. HEMA and Au were chosen for the scaffold because they are widely used in drug delivery and tissue engineering applications.[48,49] Both materials are biocompatible and may be functionalized with biomolecules for various applications.[50−54] Although Au is widely used as a biomaterial due to its low reactivity, it can form bonds with thiols. Thus, Au can interact with proteins, including fibronectin, via cysteines. Previous reports have shown that the Arg-Gly-Asp (RGD) domain of fibronectin, which contributes significantly to cellular adhesion, is not affected.[55] Au nanoparticles have been used successfully in many biological applications.[56,57]

Conductive scaffolds prepared from PANI[58,59] and PPy[8,60,61] lack the ability to easily tune their surface chemistry and mechanical properties. PANI and PPy scaffolds are opaque, which hinders visual examination during cell culture. PPy-doped scaffolds have a range of mechanical (0.5−70 MPa) and electrical (0.7−30 S/m) properties.[38,62] However, aggregation of PPy

dx.doi.org/10.1021/nl201514a |*Nano Lett.* 2011, 11, 3643–3648

particles have resulted in heterogeneous properties. We have prepared hybrid scaffolds with homogeneously distributed Au nanoparticles of uniform size. Optimization of hybrid scaffolds with tunable properties may be broadly useful in cardiac,[63,64] neuronal,[65] muscle,[66] and bone[67] tissue engineering.

In summary, we have synthesized and characterized a series of electrically conductive scaffolds based on Au impregnated thiol-HEMA/HEMA scaffolds. We demonstrated that conductive and mechanical properties may be controlled via the scaffold formulation. These novel scaffolds produce a unique cellular microenvironment that couples tunable conductivity and elasticity. Cardiomyocytes adhered and maintained viability for 8 days. Notably, Cx43 was upregulated under stimulated conditions and when seeded on conductive scaffolds in the absence of electrical stimulation. The effect of these parameters suggested that conductive scaffolds may facilitate cardiomyocyte function. Efforts to utilize electrical stimulation to regulate cell function may not be necessary. Therapeutic opportunities may exist in increasing the conductivity of damaged cardiac tissue by amplifying cell−cell communication. Tissue replacement and/or repair strategies hinge on understanding cell−matrix and, in this case, cell−electrical interactions.

■ ASSOCIATED CONTENT

Supporting Information. Details of experimental procedures, thermogravimetric analysis of Au impregnated HEMA scaffolds at different thiol−HEMA ratios (Table S1), properties of various materials used in tissue engineering (Table S2), and movie displaying cardiomyocyte beating on a three-dimensional thiol−HEMA/HEMA scaffold. This material is available free of charge via the Internet at http://pubs.acs.org.

■ AUTHOR INFORMATION

Corresponding Author

*E-mail: auguste@seas.harvard.edu.

■ ACKNOWLEDGMENT

The authors thank Professor Kevin Parker for providing neonatal rat cardiomyocytes. We gratefully acknowledge financial support from the Kavli Institute for Bionano Science and Technology at Harvard University. This work was supported primarily by the MRSEC program of the National Science Foundation under Award Number DMR-0820484. This work was performed in part at the Center for Nanoscale Systems (CNS), a member of the National Nanotechnology Infrastructure Network (NNIN), which is supported by the National Science Foundation under NSF award no. ECS-0335765. CNS is part of the Faculty of Arts and Sciences at Harvard University. We would like to thank Dr. Praveen Arany and Dr. Sotirios Banakos for critical discussions and assistance with Western blot techniques and analysis.

■ REFERENCES

(1) Gutstein, D. E.; Morley, G. E.; Tamaddon, H.; Vaidya, D.; Schneider, M. D.; Chen, J.; Chien, K. R.; Stuhlmann, H.; Fishman, G. I. *Circ. Res.* **2001**, *88*, 333.

(2) Chen, Q. Z.; Bismarck, A.; Hansen, U.; Junaid, S.; Tran, M. Q.; Harding, S. E.; Ali, N. N.; Boccaccini, A. R. *Biomaterials* **2008**, *29*, 47.

(3) Discher, D. E.; Janmey, P.; Wang, Y. L. *Science* **2005**, *310*, 1139.

(4) Engler, A. J.; Griffin, M. A.; Sen, S.; Bonnemann, C. G.; Sweeney, H. L.; Discher, D. E. *J. Cell Biol.* **2004**, *166*, 877.

(5) Huebsch, N.; Arany, P. R.; Mao, A. S.; Shvartsman, D.; Ali, O. A.; Bencherif, S. A.; Rivera-Feliciano, J.; Mooney, D. J. *Nat. Mater.* **2010**, *9*, 518.

(6) Engelmayr, G. C., Jr.; Cheng, M.; Bettinger, C. J.; Borenstein, J. T.; Langer, R.; Freed, L. E. *Nat. Mater.* **2008**, *7*, 1003.

(7) Black, L. D., 3rd; Meyers, J. D.; Weinbaum, J. S.; Shvelidze, Y. A.; Tranquillo, R. T. *Tissue Eng., Part A* **2009**, *15*, 3099.

(8) Shi, G.; Rouabhia, M.; Wang, Z.; Dao, L. H.; Zhang, Z. *Biomaterials* **2004**, *25*, 2477.

(9) Shi, G.; Rouabhia, M.; Meng, S.; Zhang, Z. *J. Biomed. Mater. Res., Part A* **2008**, *84*, 1026.

(10) Durgam, H.; Sapp, S.; Deister, C.; Khaing, Z.; Chang, E.; Luebben, S.; Schmidt, C. E. *J. Biomater. Sci., Polym. Ed.* **2010**, *21*, 1265.

(11) Schmidt, C. E.; Shastri, V. R.; Vacanti, J. P.; Langer, R. *Proc. Natl. Acad. Sci. U.S.A.* **1997**, *94*, 8948.

(12) Yamada, M.; Tanemura, K.; Okada, S.; Iwanami, A.; Nakamura, M.; Mizuno, H.; Ozawa, M.; Ohyama-Goto, R.; Kitamura, N.; Kawano, M.; Tan-Takeuchi, K.; Ohtsuka, C.; Miyawaki, A.; Takashima, A.; Ogawa, M.; Toyama, Y.; Okano, H.; Kondo, T. *Stem Cells* **2007**, *25*, 562.

(13) Chen, M. Q.; Xie, X.; Wilson, K. D.; Sun, N.; Wu, J. C.; Giovangrandi, L.; Kovacs, G. T. *Cell. Mol. Bioeng.* **2009**, *2*, 625.

(14) Park, H.; Radisic, M.; Lim, J. O.; Chang, B. H.; Vunjak-Novakovic, G. *In Vitro Cell. Dev. Biol.: Anim.* **2005**, *41*, 188.

(15) Li, M.; Guo, Y.; Wei, Y.; MacDiarmid, A. G.; Lelkes, P. I. *Biomaterials* **2006**, *27*, 2705.

(16) Jeong, S. I.; Jun, I. D.; Choi, M. J.; Nho, Y. C.; Lee, Y. M.; Shin, H. *Macromol. Biosci.* **2008**, *8*, 627.

(17) Lee, J. W.; Serna, F.; Schmidt, C. E. *Langmuir* **2006**, *22*, 9816.

(18) Hussain, I.; Graham, S.; Wang, Z.; Tan, B.; Sherrington, D. C.; Rannard, S. P.; Cooper, A. I.; Brust, M. *J. Am. Chem. Soc.* **2005**, *127*, 16398.

(19) Creighton, J. A.; Blatchford, C. G.; Albrecht, M. G. *J. Chem. Soc., Faraday Trans. 2* **1979**, *75*, 790.

(20) Freeman, R. G.; Gravar, K. C.; Allison, K. J.; Bright, R. M.; Davis, J. A.; Guthrie, A. P.; Hommer, M. B.; Jackson, M. A.; Smith, P. C.; Walter, D. G.; Natan, M. J. *Science* **1995**, *267*, 1629.

(21) Wang, C.; Flynn, N. T.; Langer, R. *Adv. Mater.* **2004**, *16*, 1074.

(22) Bhana, B.; Iyer, R. K.; Chen, W. L.; Zhao, R.; Sider, K. L.; Likhitpanichkul, M.; Simmons, C. A.; Radisic, M. *Biotechnol. Bioeng.* **2010**, *105*, 1148.

(23) Shapira-Schweitzer, K.; Seliktar, D. *Acta Biomater.* **2007**, *3*, 33.

(24) Jalil, J. E.; Doering, C. W.; Janicki, J. S.; Pick, R.; Shroff, S. G.; Weber, K. T. *Circ. Res.* **1989**, *64*, 1041.

(25) Boublik, J.; Park, H.; Radisic, M.; Tognana, E.; Chen, F.; Pei, M.; Vunjak-Novakovic, G.; Freed, L. E. *Tissue Eng.* **2005**, *11*, 1122.

(26) Mirsky, I.; Parmley, W. W. *Circ. Res.* **1973**, *33*, 233.

(27) Phillips, C. A.; Petrofsky, J. S. *J. Biomech.* **1984**, *17*, 561.

(28) Westerhof, N.; Stergiopulos, N.; Noble, M. I. M. *Snapshots of Hemodynamics: An Aid for Clinical Research and Graduate Education*, 2nd ed.; Springer: New York, 2010.

(29) Sugino, T.; Kiyohara, K.; Takeuchi, I.; Mukai, K.; Asaka, K. *Sens. Actuators, B* **2009**, *141*, 179.

(30) Jun, I.; Jeong, S.; Shin, H. *Biomaterials* **2009**, *30*, 2038.

(31) Gelmi, A.; Higgins, M. J.; Wallace, G. G. *Biomaterials* **2010**, *31*, 1974.

(32) Yow, S. Z.; Lim, T. H.; Yim, E. K. F.; Lim, C. T.; Leong, K. W. *Polymers* **2011**, *3*, 527.

(33) Yost, M. J.; Baicu, C. F.; Stonerock, C. E.; Goodwin, R. L.; Price, R. L.; Davis, J. M.; Evans, H.; Watson, P. D.; Gore, C. M.; Sweet, J.; Creech, L.; Zile, M. R.; Terracio, L. *Tissue Eng.* **2004**, *10*, 273.

(34) Parker, K. K.; Tan, J.; Chen, C. S.; Tung, L. *Circ. Res.* **2008**, *103*, 340.

(35) McDevitt, T. C.; Woodhouse, K. A.; Hauschka, S. D.; Murry, C. E.; Stayton, P. S. *J. Biomed. Mater. Res., Part A* **2003**, *66*, 586.

(36) You, J. O.; Auguste, D. T. *Langmuir* **2010**, *26*, 4607.

(37) Zhao, X.; Ding, X.; Deng, Z.; Zheng, Z.; Peng, Y.; Long, X. *Macromol. Rapid Commun.* **2005**, *26*, 1784.

(38) Wan, Y.; Yu, A. X.; Wu, H.; Wang, Z. X.; Wen, D. J. *J. Mater. Sci.: Mater. Med.* **2005**, *16*, 1017.
(39) Potse, M.; Dube, B.; Vinet, A. *Med. Biol. Eng. Comput.* **2009**, *47*, 719.
(40) Guerrero, P. A.; Schuessler, R. B.; Davis, L. M.; Beyer, E. C.; Johnson, C. M.; Yamada, K. A.; Saffitz, J. E. *J. Clin. Invest.* **1997**, *99*, 1991.
(41) Oyamada, M.; Kimura, H.; Oyamada, Y.; Miyamoto, A.; Ohshika, H.; Mori, M. *Exp. Cell Res.* **1994**, *212*, 351.
(42) Ando, M.; Katare, R. G.; Kakinuma, Y.; Zhang, D.; Yamasaki, F.; Muramoto, K.; Sato, T. *Circulation* **2005**, *112*, 164.
(43) Bupha-Intr, T.; Haizlip, K. M.; Janssen, P. M. *Am. J. Physiol.: Heart Circ. Physiol.* **2009**, *296*, H806.
(44) Radisic, M.; Park, H.; Shing, H.; Consi, T.; Schoen, F. J.; Langer, R.; Freed, L. E.; Vunjak-Novakovic, G. *Proc. Natl. Acad. Sci. U.S.A.* **2004**, *101*, 18129.
(45) Gaudet, C.; Marganski, W. A.; Kim, S.; Brown, C. T.; Gunderia, V.; Dembo, M.; Wong, J. Y. *Biophys. J.* **2003**, *85*, 3329.
(46) Liu, L.; Ratner, B. D.; Sage, E. H.; Jiang, S. *Langmuir* **2007**, *23*, 11168.
(47) Cavalcanti-Adam, E. A.; Volberg, T.; Micoulet, A.; Kessler, H.; Geiger, B.; Spatz, J. P. *Biophys. J.* **2007**, *92*, 2964.
(48) West, J. L.; Halas, N. J. *Curr. Opin. Biotechnol.* **2000**, *11*, 215.
(49) Ratner, B. D.; Hoffman, A. S.; Schoen, F. J.; Lemons, J. E. *Biomaterials science: an introduction to materials in medicine*; Elsevier Academic Press: Amsterdam and Boston, MA, 2004.
(50) You, J. O.; Auguste, D. T. *Biomaterials* **2008**, *29*, 1950.
(51) You, J. O.; Auguste, D. T. *Nano Lett.* **2009**, *9*, 4467.
(52) Gulsen, D.; Chauhan, A. *Int. J. Pharm.* **2005**, *292*, 95.
(53) Nuzzo, R.; Allara, D. *J. Am. Chem. Soc.* **1983**, *105*, 4481.
(54) Kamei, K.; Mukai, Y.; Kojima, H.; Yoshikawa, T.; Yoshikawa, M.; Kiyohara, G.; Yamamoto, T. A.; Yoshioka, Y.; Okada, N.; Seino, S.; Nakagawa, S. *Biomaterials* **2009**, *30*, 1809.
(55) Pierschbacher, M. D.; Ruoslahti, E. *Nature* **1984**, *309*, 30.
(56) Rosi, N. L.; Giljohann, D. A.; Thaxton, C. S.; Lytton-Jean, A. K.; Han, M. S.; Mirkin, C. A. *Science* **2006**, *312*, 1027.
(57) Chithrani, B. D.; Chan, W. C. *Nano Lett.* **2007**, *7*, 1542.
(58) Liu, H.; Kameoka, J.; Czaplewski, D. A.; Craighead, H. G. *Nano Lett.* **2004**, *4*, 671.
(59) Zhang, L.; Wan, M. *Adv. Funct. Mater.* **2003**, *13*, 815.
(60) Lee, J. Y.; Lee, J. W.; Schmidt, C. E. *J. R. Soc., Interface* **2009**, *6*, 801.
(61) Mihardja, S. S.; Sievers, R. E.; Lee, R. J. *Biomaterials* **2008**, *29*, 4205.
(62) Wan, Y.; Wu, H.; Wen, D. J. *Macromol. Biosci.* **2004**, *4*, 882.
(63) Tandon, N.; Cannizzaro, C.; Chao, P. H.; Maidhof, R.; Marsano, A.; Au, H. T.; Radisic, M.; Vunjak-Novakovic, G. *Nat. Protoc.* **2009**, *4*, 155.
(64) Durand, D. In *The Biomedical Engineering Handbook*; Durand, D., Bronzino, J. D., Eds.; CRC Press: Boca Raton, FL, 1995; p 229.
(65) Hoppe, D.; Chvatal, A.; Kettenmann, H.; Orkand, R. K.; Ransom, B. R. *Brain Res.* **1991**, *552*, 106.
(66) Cannizzaro, C.; Tandon, N.; Figallo, E.; Park, H.; Gerecht, S.; Radisic, M.; Elvassore, N.; Vunjak-Novakovic, G. *Principles of Tissue Engineering*, 2nd ed.; Elsevier Academic Press: Amsterdam and Boston, MA, 2008.
(67) De Giglio, E.; Sabbatini, L.; Zambonin, P. G. *J. Biomater. Sci., Polym. Ed.* **1999**, *10*, 845.